Optical and transmission-electron-microscopy characterization of metal precipitates in doped thermochemically reduced magnesium oxide

C. Ballesteros and R. González
Departamento de Física del Estado Sólido, Facultad de Ciencias Físicas, Universidad Complutense, 28040 Madrid, Spain

Y. Chen
Solid State Division, Oak Ridge National Laboratory, Oak Ridge, Tennessee 37831-6061
(Received 31 July 1987)

MgO crystals doped with Co, Cu, and V were thermochemically reduced at high temperatures. Changes in coloration were observed in all these crystals due to broad optical extinction bands in the visible region. These bands are impurity related. Analytical transmission-electron-microscopy techniques indicated the presence of metallic precipitates consisting of Co in the Co-doped sample, Cu with some precipitates of Fe in the Cu-doped sample, and a V-Fe-Cr alloy in the V-doped sample. Microdiffraction patterns indicated that the Co precipitates possessed the fcc ($a_0 = 3.54$ Å) crystal structure and V-Fe-Cr alloy precipitates showed a bcc ($a_0 = 2.89$ Å) crystal structure.

I. INTRODUCTION

Metallic precipitates or colloids with particle sizes of 1–200 nm in ionic crystals are known to produce important modifications of mechanical, electrical, and other properties, making them suitable for high technology applications.[1] Selective absorption of solar energy, and cathodochromic, photochromic and data storage applications are a few examples of the modification of physical properties produced by colloids in insulators.[1]

Recently, a method based on thermochemical reduction (TCR) has been developed to produce a fairly uniform concentration of metal precipitates or colloids in oxides.[2] Other methods which result in precipitates involve ion implantation with subsequent heat treatment,[3] and electrolytical coloration at elevated temperatures.[4] After TCR, the appearance of precipitates is a general feature in nominally pure and doped MgO crystals.[5–7] This paper describes our optical and analytical transmission-electron-microscopy (TEM) studies of precipitates in MgO single crystals each doped with Co, Cu, and V.

II. EXPERIMENTAL PROCEDURES

Magnesium oxide crystals doped with cobalt or copper were grown at the Oak Ridge National Laboratory by an arc-fusion technique[8] using high-purity MgO powder from Kanto Chemical Chemistry, Tokyo, Japan. Magnesium oxide crystals doped with vanadium were grown by the Tateho Chemical Company, Japan. The dopant concentration was determined by neutron activation analysis, with an accuracy of ±5%, to be ~2100 ppm of cobalt, ~40 ppm of copper, and ~350 ppm of vanadium for the three doped crystals. The total background impurity of undoped MgO crystals is about 50 ppm for the Oak Ridge National Laboratory crystals[8–10] and higher for the Tateho Chemical Company crystals.

Single-crystal samples having {100} faces with typical dimensions $\sim 1 \times 1 \times 0.1$ cm^3 were enclosed in an evacuated tantalum chamber containing magnesium vapor, heated to temperatures of about 2000 K and then cooled. The samples for electron microscopy were prepared by a jet polishing technique using phosphoric acid at 410 K. Philips 420 and JEOL 100 U transmission-electron microscopes were used in this investigation.

The x-ray microanalysis and the diffraction studies of individual precipitates were carried out in a Philips 420 analytical electron microscope. The twin lens design results in electron probe diameters as small as 10 nm in microprobe mode. Thus, it is possible to obtain diffraction information (hereafter designated as micro-micro diffraction) from areas significantly smaller than the ~300 nm diameter required in the selected-area diffraction technique used in a conventional transmission-electron microscope.[11]

Near-infrared, visible, and uv measurements were made in a Perkin-Elmer, Lambda 9 spectrophotometer. Luminescence experiments were performed in a Spex Industries Fluorometer Model 212. High-temperature heat treatments were performed in a Lindberg 5400 Series furnace.

III. RESULTS AND DISCUSSION

A. Optical measurements

1. *Absorption spectra*

Thermochemical reduction of doped MgO crystals results in a dark coloration in the crystals due to extinction in the visible region. These broad extinctions have been associated with Mie scattering from precipitates generated during the TCR process. We characterized the optical spectra before and after TCR for each of the three types of doped crystals.

a. MgO:Co crystals. The optical-absorption spectrum

of a Co-doped MgO sample before thermochemical reduction is shown in Fig. 1(a). In the as-grown crystal, two bands appear at ~ 2.4 and ~ 4.3 eV. Their full widths at half maximum (FWHM's) are ~ 0.3 and ~ 0.5 eV, respectively. The former band has been attributed to $d \rightarrow d$ transitions of Co^{2+} ions,[12] and the latter to the Fe^{3+} charge transfer band.[13,14] As evidence for the latter identification, oxidation for 30 min at 1773 K increased the band intensity [Fig. 1(b)] and reduction for 30 min at 1773 K almost annealed out the 4.3-eV band [Fig. 1(c)], indicating that Fe^{3+} ions were converted into Fe^{2+} ions during the reduction treatment. The Fe^{3+} concentration in the oxidized state can be estimated[15] to be ~ 60 ppm, as compared to the 2100 ppm of Co^{2+} ions. In contrast, the 2.4-eV band remains almost unchanged after oxidation and slightly diminished after reduction.

The initial pink coloration of these crystals turned dark and almost opaque after TCR at ~ 2000 K. A broad and intense extinction was observed near 3.7 eV (Fig. 2).

b. MgO:Cu crystals. Figure 3 shows the optical-absorption spectra of a cooper-doped MgO sample before and after TCR at ~ 2000 K. In the as-grown crystal, substitutional Cu ions produced absorption bands of about equal intensity at 5.5 and 4.5 eV, with FWHM of about 0.6 eV. After TCR the intensity of these two bands increased and a very broad extinction emerged at 3.0 eV. The initially transparent crystals acquired a reddish coloration after TCR.

c. MgO:V crystals. Figure 4 shows the optical-absorption spectra of a V-doped MgO sample before and after TCR. In the as-grown crystal, an intense absorption band at 5.15 eV is observed [Fig. 4(a)]. This band has been previously assigned to an electronic transition from an orbital predominantly on the oxygen ligands of the V^{3+} ion to an orbital predominantly on the V^{3+} ion.[16] In addition, two weak bands at 2.9 and 2.0 eV appeared (inset). These bands in the visible region were assigned to transitions within the Stark-split d shell of the V^{3+} ion. After TCR the V^{3+} bands were not apparent. Instead, a band at 5.0 eV and another very broad band centered at about 3.5 eV were observed. The former band is due to anion vacancies.[17]

In Fig. 5, we illustrate the spectra before and after oxidation at 1773 K for 30 min. Oxidation did not significantly modify the intensity of the vanadium bands. However, Fe^{3+} absorption bands at 4.3 and 5.7 eV experienced a large increase. From the absorption coefficient of the band at 4.3 eV the Fe^{3+} concentration can be estimated to be ~ 80 ppm.

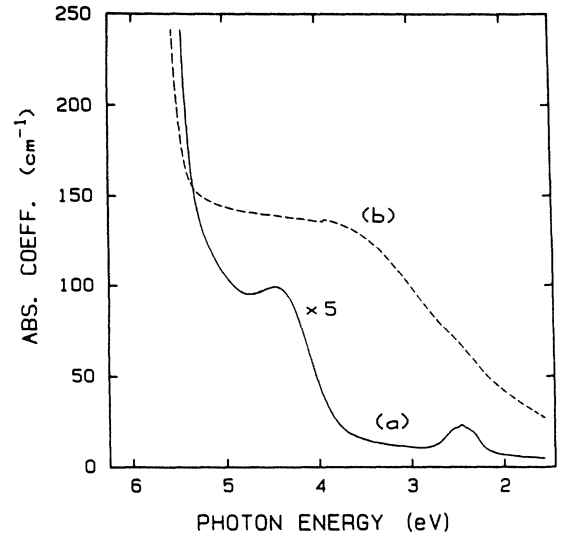

FIG. 2. Optical-absorption spectra of MgO:Co crystals (a) as-grown, (b) after thermochemical reduction at ~ 2000 K.

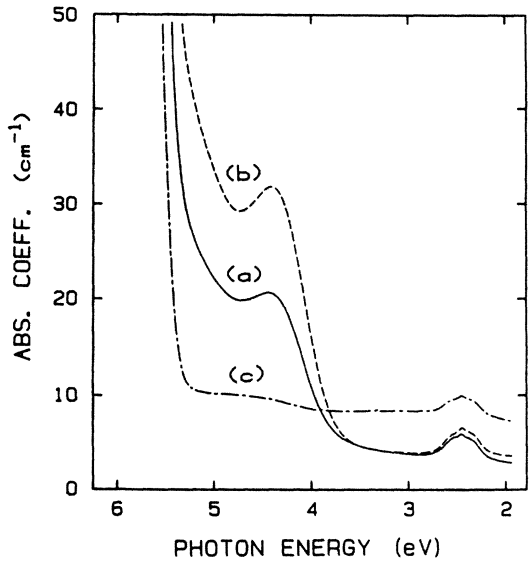

FIG. 1. Optical-absorption spectra of MgO:Co crystals (a) as-grown, (b) after oxidation at 1773 K, and (c) after reduction at 1773 K.

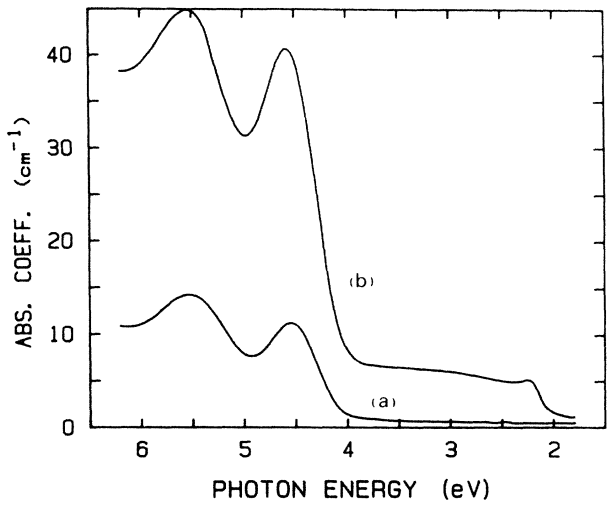

FIG. 3. Optical-absorption spectra of an as-grown MgO:Cu crystal (bottom) and of a thermochemically reduced MgO:Cu crystal (top).

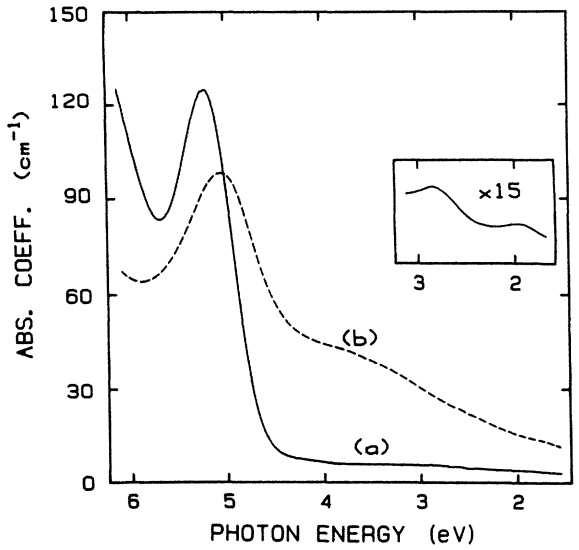

FIG. 4. Optical-absorption spectra of MgO:V crystals, (a) as-grown, and (b) after thermochemical reduction. In the inset the bands at 2.9 and 2.0 eV are magnified 15× in the vertical direction for the as-grown crystal.

2. *Luminescence spectra*

In as-grown MgO crystals doped with Co, Cu, or V, photoluminescence experiments show that when these crystals are excited in the impurity absorption bands reported in Sec. III A 1 no luminescence emission has been detected in the region between 300 and 750 nm. However, the characteristic Cr^{3+} luminescence was observed when the crystals were excited in the Cr^{3+}-absorption region at 2.8 eV.[18] The emission intensity was low in the two types of crystals grown at Oak Ridge (MgO:Co and MgO:Cu) and higher in the Tateho crystals (MgO:V) indicating that the Cr^{3+} content in the Oak Ridge Crystals was lower than that in Tateho crystals.

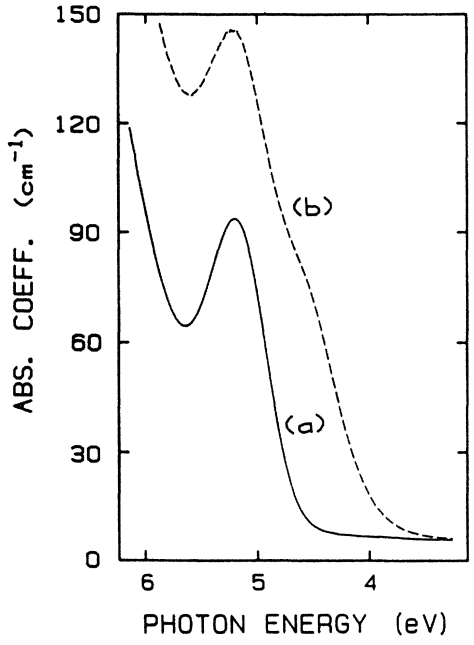

FIG. 5. Optical-absorption spectra of MgO:V crystals, (a) as-grown, (b) after oxidation at 1773 K.

B. Transmission-electron-microscopy observations

After TCR at ~2000 K, the samples exhibit broad extinction in the visible part of the spectrum. The reduction was found to initiate from the surface of the specimens and the concentration of precipitates was higher in the surface region. Electron microscopy observations indicated that in all the specimens the distribution of precipitates was very inhomogeneous. Areas with a high concentration of precipitates were separated by regions which were almost free from precipitates. For this reason, the total precipitate concentration was not measured. In addition to precipitates, dislocations and dislocation loops with sizes up to ~500 nm were imaged as previously found in undoped MgO.[7]

1. *MgO:Co crystals*

Figure 6 shows a typical electron micrograph from a region with a high concentration of precipitates in a TCR cobalt-doped MgO specimen. The black spots are due to precipitates. The average size was determined to be 100 nm. Often the precipitates appear following irregular lines that could be associated to dislocations (Fig. 7). High magnification micrographs showed that the shape of the precipitates was not always well defined (Fig. 8).

The structure of the precipitates was investigated by microdiffraction techniques. Microdiffraction with a

FIG. 6. Electron micrograph showing the cobalt precipitates in a MgO:Co specimen.

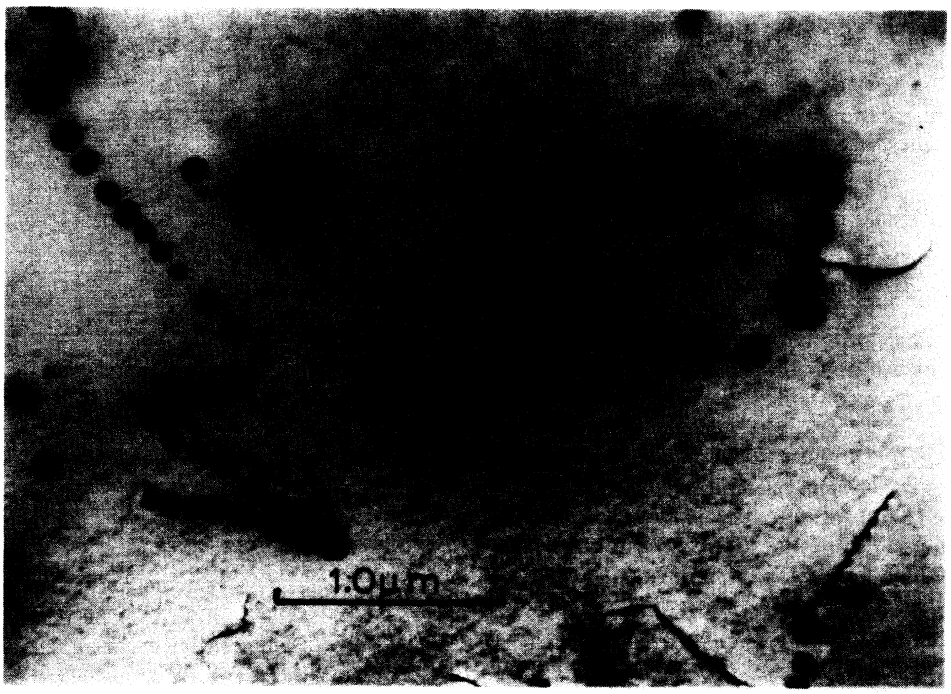

FIG. 7. Electron micrograph of aligned cobalt precipitates in a MgO:Co specimen.

finite incident divergence produces diffraction patterns which consist of disks. A pattern of this type, shown in Fig. 9, was obtained from a precipitate embedded in the matrix. It therefore contained matrix as well as precipitate reflections, and from a number of such patterns the crystallographic relationship between the matrix and the precipitate was determined. Using the MgO matrix spots as an internal calibration, the precipitate reflections were found to correspond to a fcc crystal structure with a lattice constant of $a_0 = 3.55 \pm 0.01$ Å, essentially the same as that of bulk fcc cobalt in the β phase. The cobalt hexagonal phase was not observed. The following crystallographic relationship between matrix and precipitates was found:

$$\text{fcc } \langle 001 \rangle_p \| \langle 001 \rangle_m \ ,$$

and

$$\langle 010 \rangle_p \| \langle 010 \rangle_m \ .$$

FIG. 8. Electron micrograph of cobalt precipitates with a poorly defined shape in a MgO:Co specimen.

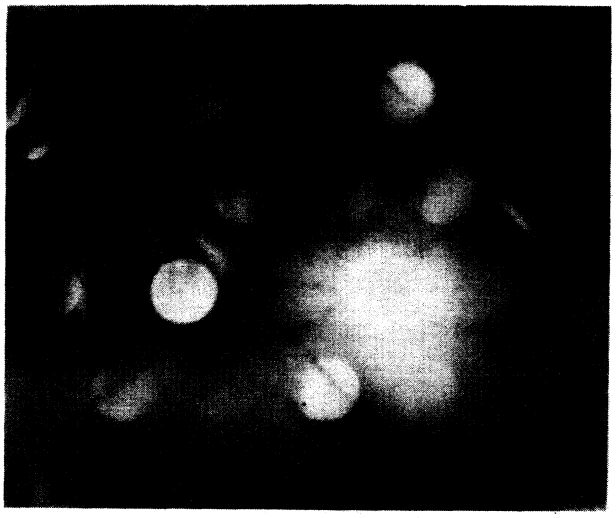

FIG. 9. Microdiffraction pattern from a fcc cobalt precipitate in a MgO:Co specimen.

X-ray microanalysis was also performed on precipitates near the edge of the specimen using the small convergent probe. Figure 10 shows a typical x-ray fluorescence spectrum from the precipitate exhibiting the Co $K\alpha$ and Co $K\beta$ lines. No iron signal was detected, in agreement with the optical observation that the iron concentration was much smaller than the cobalt concentration in the crystals.

2. *MgO:Cu crystals*

In thermochemically reduced MgO:Cu crystals, the precipitate concentration was very small, in agreement with the small impurity content of these samples. Figure 11 shows an electron micrograph from one of the regions of the crystal with the highest concentration of precipitates. The average size of the precipitates was also small, about 10 nm. Microdiffraction patterns from some of the largest precipitates showed that these precipitates were incoherent and have a fcc crystal structure with a lattice constant of $a_0 = 3.63 \pm 0.03$ Å, close to that of bulk fcc copper. X-ray microanalysis of the precipitates indicated that most of the precipitates were indeed due to copper (Fig. 12), although some iron precipitates were also found. Iron precipitates and Fe-Cr precipitates have been previously found in undoped MgO after TCR.[7] The fact that individual Cu and Fe precipitates have been observed, but not Cu-Fe precipitates, is probably a consequence of the low solid solubility of Fe in Cu, which is at most several percent.[19] There are no intermediate phases in the Cu-Fe system.[19]

3. *MgO:V crystals*

Electron microscopy studies of MgO:V crystals after TCR showed the presence of precipitates. These precipitates had an average size of about 40 nm and a concentration intermediate between those of MgO:Co and MgO:Cu

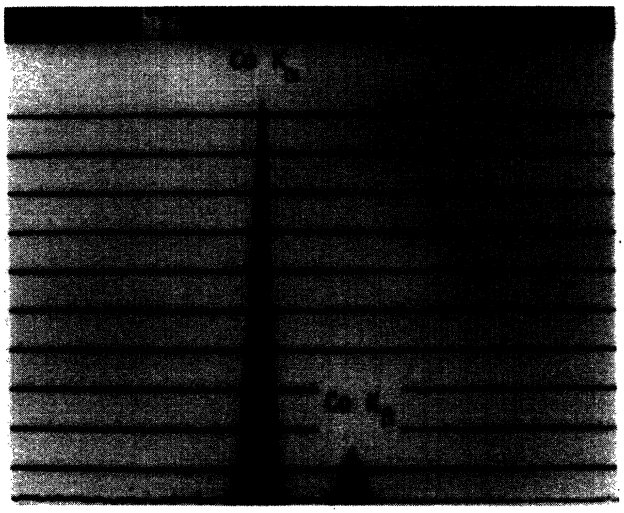

FIG. 10. Energy-dispersive x-ray fluorescence spectrum from a Co precipitate showing the Co $K\alpha$ and Co $K\beta$ peaks.

FIG. 11. Electron micrograph showing the copper precipitates in a MgO:Cu specimen.

(Fig. 13). Microdiffraction patterns indicate that the reflections associated with the precipitates correspond to a bcc crystal structure with a lattice constant of $a_0 = 2.89 \pm 0.01$ Å, which is close to that of bulk bcc V-Fe-Cr solid solutions.[19] The following crystallographic relationship between matrix and precipitates was found:

$$\text{bcc } \langle 100 \rangle_p \| \langle 100 \rangle_m ,$$

and

$$\langle 110 \rangle_p \| \langle 010 \rangle_m .$$

X-ray microanalysis of the precipitates indicated the presence of V, Fe, and Cr. Figure 14 shows a typical x-ray fluorescence spectrum from the precipitates. It exhibits the V $K\alpha$ and V $K\beta$ lines, the Cr $K\alpha$ and Cr $K\beta$ lines and the Fe $K\alpha$ and Fe $K\beta$ lines. The V $K\beta$ line and the Cr $K\alpha$ line overlapped. The relative concentrations of the three impurities were analyzed using x-ray generation constants computed by a standardless method.[20]

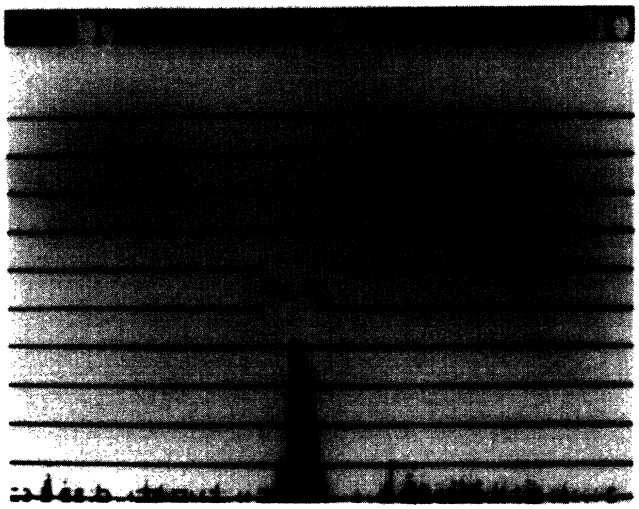

FIG. 12. Energy-dispersive x-ray fluorescence spectrum from a Cu precipitate showing the Cu $K\alpha$ peak.

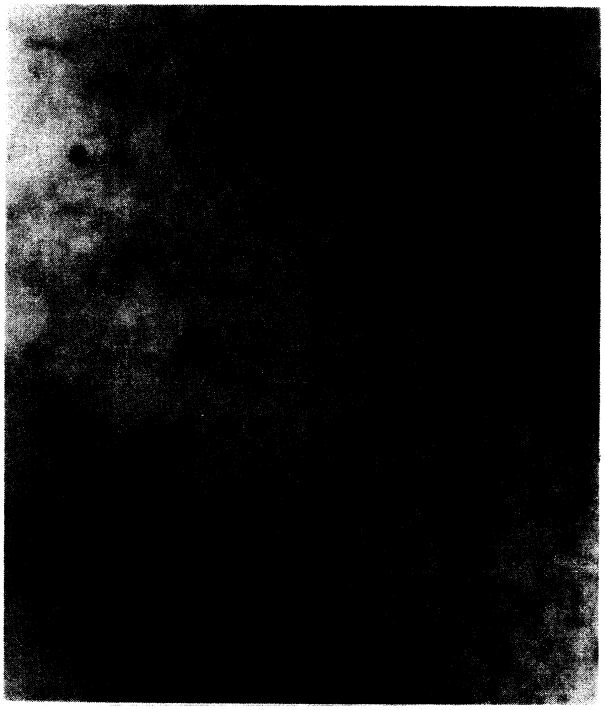

FIG. 13. Electron micrograph showing the precipitates in a MgO:V specimen.

FIG. 14. Energy-dispersive x-ray fluorescence spectrum from a V-Fe-Cr precipitate showing the V $K\alpha$ and V $K\beta$ lines, the Cr $K\alpha$ and Cr $K\beta$ lines and the Fe $K\alpha$ and Fe $K\beta$ lines.

The concentration of vanadium in the precipitates was $\sim 55\%$, iron $\sim 40\%$, and chromium $\sim 5\%$. The chromium concentration was not very accurate since its $K\alpha$ line overlapped with the V $K\beta$ line. The large iron content in these precipitates is not surprising since the optical-absorption spectrum of an oxidized crystal shows indeed the presence of iron.

IV. SUMMARY AND CONCLUSIONS

MgO single crystals doped with Co, Cu, and V were thermochemically reduced at high temperatures. Broad optical extinction bands in the visible region were observed in all these crystals. They were responsible for the dark coloration of the sample. The coloration after TCR depended on the impurity content of the crystal. Optical and analytical transmission-electron-microscopy studies showed that the coloration was due to Mie scattering from metallic precipitates in the crystals. The precipitates were characterized using analytical transmission-electron microscopy. The greater the transition-metal impurity content the larger were the dimension and number density of the precipitates.

In MgO:Co crystals, cobalt precipitates 100 nm in average size were observed. The precipitates possess the fcc structure, with a lattice constant of $a_0 = 3.54 \pm 0.01$ Å and a $\langle 001 \rangle_p \| \langle 001 \rangle_m$ and $\langle 010 \rangle_p \| \langle 010 \rangle_m$ precipitate-matrix orientation relationship.

Incoherent copper precipitates with an average size of 10 nm and a fcc crystal structure were imaged in MgO:Cu crystals. The lattice constant was determined to be $a_0 = 3.63 \pm 0.03$ Å. In these crystals iron precipitates were also observed, but no Cu-Fe alloys were found.

In MgO:V crystals, V-Fe-Cr precipitates were studied. The precipitates with an average size of 40 nm exhibited a bcc crystal structure with a lattice constant of 2.89 ± 0.01 Å. The precipitates have a $\langle 100 \rangle_p \| \langle 100 \rangle_m$ and $\langle 110 \rangle_p \| \langle 010 \rangle_m$ precipitate-matrix relationship.

ACKNOWLEDGMENTS

The authors are indebted to M. M. Abraham for his assistance in the growth of the Oak Ridge National Laboratory crystals and to M. A. Ollacarizqueta of the Servicio de Microscopía Electrónica Analítica del Centro de Investigaciones Biológicas for her assistance in the use of the electron microscope. We also thank S. J. Pennycook for a critical reading of the manuscript. This research was supported by the Comisión Asesora de Investigación Científica y Técnica of Spain, and by the Division of Materials Sciences, Office of Basic Energy Sciences, U. S. Department of Energy, under Contract No. DE-AC05-84OR21400 with Martin Marietta Energy Systems, Inc.

[1] A. E. Hughes and S. C. Jain, Adv. Phys. **28**, 171 (1979).

[2] J. Narayan, Y. Chen, and R. M. Moon, Phys. Rev. Lett. **46**, 1491 (1981).

[3] M. Treilleux and G. Chassange, J. Phys. (Paris) Lett. **40**, L161 (1979).

[4] M. M. Abraham, L. A. Boatner, W. H. Christie, F. A. Modine, T. Negas, R. M. Bunch, and W. P. Unruh, J. Solid State Chem. **51**, 1 (1984).

[5]J. Narayan, Y. Chen. R. M. Moon, and R. N. Carpenter, Philos. Mag. A **49**, 287 (1984).
[6]R. M. Bunch, W. P. Unruh, and M. V. Iverson, J. Appl. Phys. **58**, 1474 (1985).
[7]C. Ballesteros, R. González, S. J. Pennycook, and Y. Chen (unpublished).
[8]M. M. Abraham, C. T. Butler, and Y. Chen, J. Chem. Phys. **55**, 3752 (1979).
[9]K. L. Tsang and Y. Chen, J. Appl. Phys. **54**, 4531 (1983).
[10]Y. Chen, D. L. Trueblood, O. E. Schow, and H. T. Tohver, J. Phys. C **3**, 2501 (1970).
[11]R. W. Carpenter, J. Bentley, and E. A. Kenik, Scanning Electron Micros. **1**, 411 (1977).
[12]A. J. Mann and P. J. Stephens, Phys. Rev. B **9**, 863 (1974).
[13]R. W. Soshea, A. J. Dekker, and J. P. Sturtz, J. Phys. Chem. Solids **5**, 23 (1958).
[14]W. A. Sibley, J. L. Kolopus, and W. C. Mallard, Phys. Status Solidi **31**, 223 (1969).
[15]Y. Chen and W. A. Sibley, Phys. Rev. **154**, 842 (1967).
[16]F. A. Modine, Phys. Rev. B **8**, 854 (1973).
[17]Y. Chen, J. L. Kolopus, and W. A. Sibley, Phys. Rev. **182**, 960 (1969).
[18]D. S. McClure, J. Chem. Phys. **36**, 2757 (1962).
[19]W. B. Pearson, *Handbook of Lattice Spacings and Structures of Metals and Alloys* (Pergamon, New York, 1958), Chap. 11.
[20]N. J. Zaluzec, *Introduction to Analytical Electron Microscopy*, edited by J. Hren, J. Goldstein, and D. Joy (Plenum, New York, 1979), p. 121.

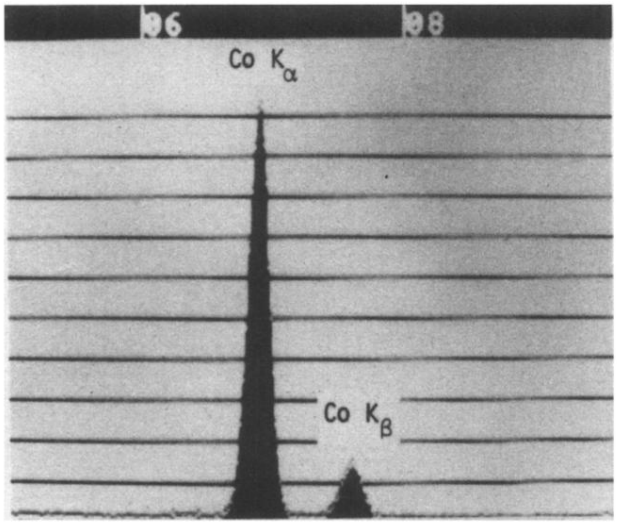

FIG. 10. Energy-dispersive x-ray fluorescence spectrum from a Co precipitate showing the Co $K\alpha$ and Co $K\beta$ peaks.

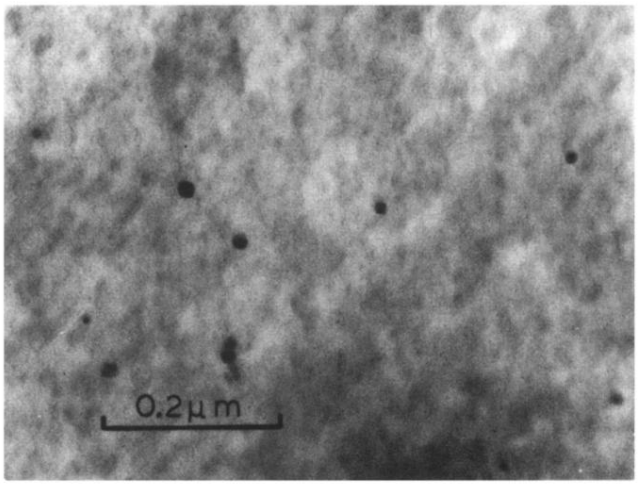

FIG. 11. Electron micrograph showing the copper precipitates in a MgO:Cu specimen.

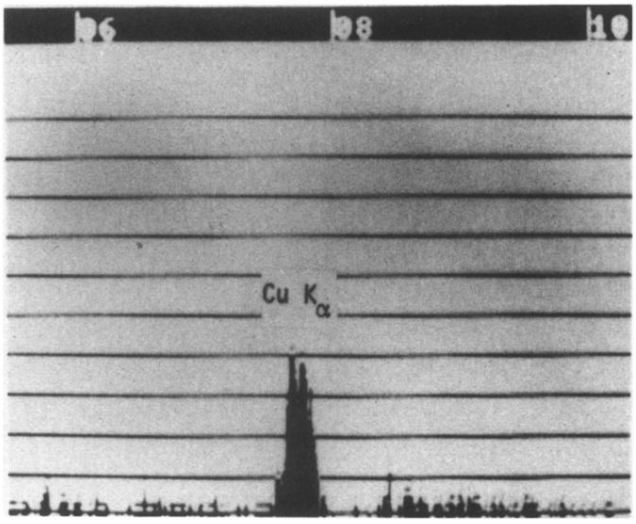

FIG. 12. Energy-dispersive x-ray fluorescence spectrum from a Cu precipitate showing the Cu $K\alpha$ peak.

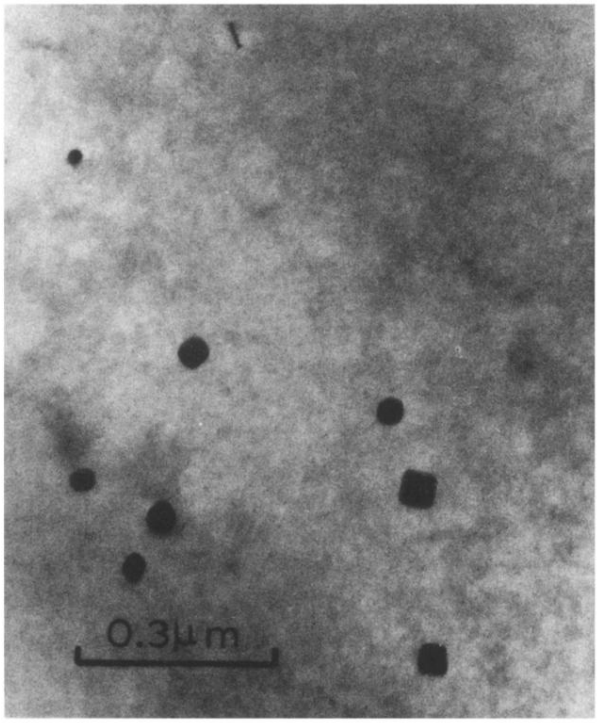

FIG. 13. Electron micrograph showing the precipitates in a MgO:V specimen.

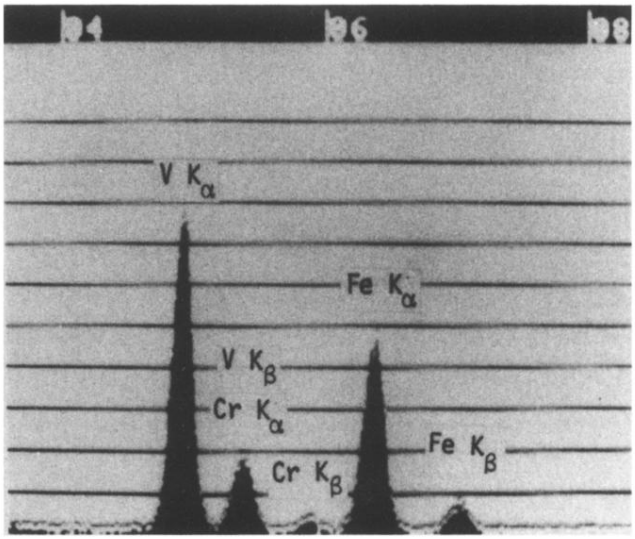

FIG. 14. Energy-dispersive x-ray fluorescence spectrum from a V-Fe-Cr precipitate showing the V $K\alpha$ and V $K\beta$ lines, the Cr $K\alpha$ and Cr $K\beta$ lines and the Fe $K\alpha$ and Fe $K\beta$ lines.

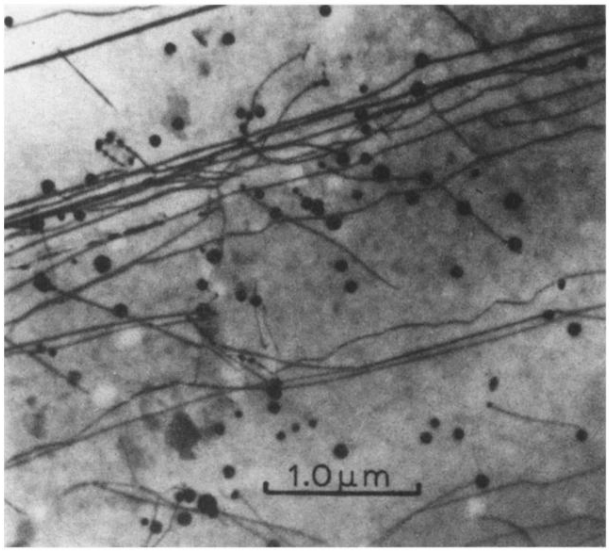

FIG. 6. Electron micrograph showing the cobalt precipitates in a MgO:Co specimen.

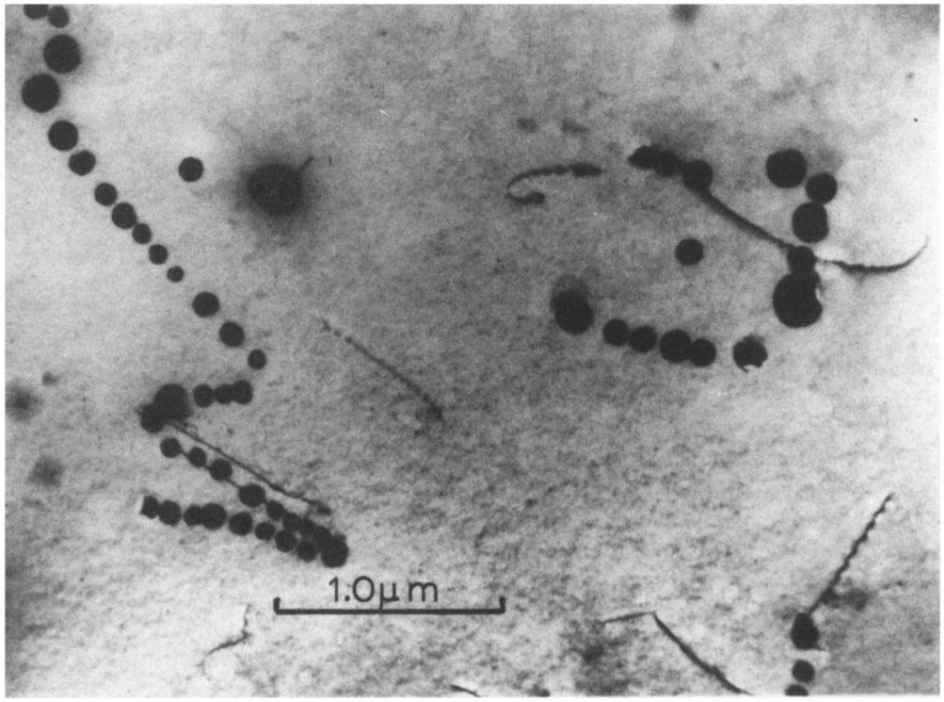

FIG. 7. Electron micrograph of aligned cobalt precipitates in a MgO:Co specimen.

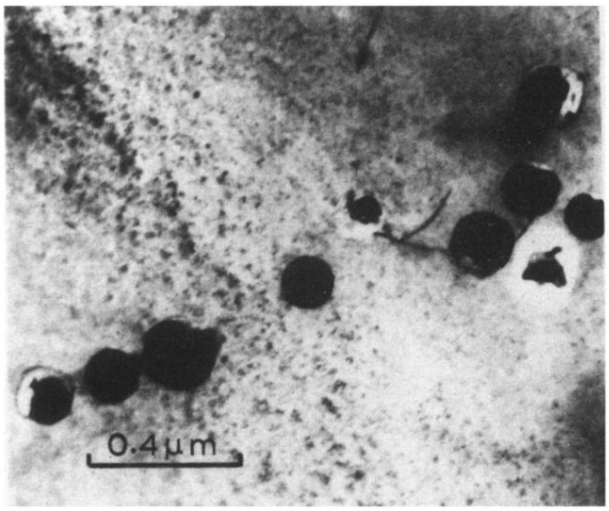

FIG. 8. Electron micrograph of cobalt precipitates with a poorly defined shape in a MgO:Co specimen.

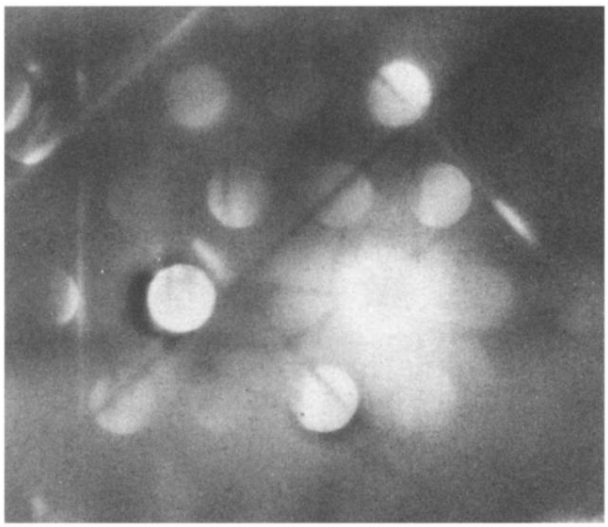

FIG. 9. Microdiffraction pattern from a fcc cobalt precipitate in a MgO:Co specimen.